Comparison of Droplet- and Microwell-based Methods to Analyze Cryopreserved Human Bronchoalveolar Lavage Cells by scRNA-Sequencing

Authors

Pierre Janssen, DVM[1,2,*], Joan Abinet, MSc[1,*], Latifa Karim[3], Wouter Coppieters, PhD[3], Catherine Moermans, DVM, PhD[4], Julien Guiot, MD, PhD[4], Florence Schleich, MD, PhD[4], Coraline Radermecker, DVM, PhD[1,2] & Thomas Marichal, DVM, PhD[1,2,5].

Affiliations

[1] Laboratory of Immunophysiology, GIGA Institute, University of Liège, Liège, Belgium

[2] Faculty of Veterinary Medicine, University of Liège, Liège, Belgium

[3] Genomic Facility, GIGA Institute, University of Liège, Liège, Belgium

[4] Laboratory of Pneumology, GIGA Institute, University of Liège, Liège, Belgium

[5] Walloon Excellence in Life Sciences and Biotechnology (WELBIO) Department, WEL Research Institute, Wavre, Belgium

[*] These authors contributed equally to this work and are co-first authors

Author contributions

TM conceived, supervised and secured funding for the project; PJ, CR and TM designed the experiments; PJ performed the experiments, compiled the data, contributed to the bioinformatic analyses and prepared the figures. JA performed the bioinformatic analyses and prepared the associated figure panels. KL and WC were involved in sample processing and sequencing. CM performed differential cell counts of the BALF cells on

AJRCMB Articles in Press. Published May 20, 2025 as 10.1165/rcmb.2024-0467MA

cytospins. JG and FS collected the BALF samples. TM and PJ wrote the manuscript; all authors provided feedback on the manuscript.

ORCID IDs: 0009-0006-2501-9463 (P.J.); 0009-0008-3551-7735 (J.A.); 0000-0001-8109-7825 (W.C.); 0000-0002-9558-5878 (C.M.); 0000-0001-7800-1730 (F.S.); 0000-0001-6254-5258 (C.R.); 0000-0003-1688-6291 (T.M.).

Correspondence

Thomas Marichal

Laboratory of Immunophysiology,

GIGA Institute, University of Liège,

Quartier Hôpital, B34,

Avenue de l'Hôpital 11,

4000 Liege, Belgium

t.marichal@uliege.be

Artificial Intelligence Disclaimer: No artificial intelligence tools were used in writing this manuscript.

This article has a data supplement, which is accessible at the Supplements tab.

AJRCMB Articles in Press. Published May 20, 2025 as 10.1165/rcmb.2024-0467MA

Abstract

Single-cell and single-nuclei RNA sequencing (scRNA-seq) has revolutionized the exploration of tissue biology and cellular heterogeneity by delivering transcriptomic data at the individual cell level. Yet, the logistical challenge of utilizing fresh material has hindered investigations, particularly on human samples. Here, we aimed to address this limitation by implementing and comparing two cryopreservation and scRNA-seq methods for human bronchoalveolar lavage fluid (BALF) cells based on droplet and microwell entrapment. Four BALF samples were collected from routine diagnostic procedures and each sample was divided and processed using both techniques. Although the droplet-based method initially required a greater number of cells for fixation and cryopreservation, cells recovered post-sequencing and quality filtering displayed significantly higher counts of transcripts and genes per cell. This was particularly evident for alveolar macrophages, epithelial cells, mast cells and T cells, while both methodologies were similarly able to capture transcripts from neutrophils. Of note, the microwell-based approach uniquely identified fragile eosinophils. We performed single cell regulatory network inference and clustering (SCENIC) analyses and found that the ability to predict the activities of key transcription factors implicated in the differentiation and identity of BALF immune cells populations correlated with the amounts of transcripts and genes per cell. Our results can serve as a resource for the design of large-scale translational and clinical projects involving scRNA-seq analyses.

AJRCMB Articles in Press. Published May 20, 2025 as 10.1165/rcmb.2024-0467MA

Introduction

Single-cell and single-nuclei RNA sequencing (scRNA-seq) technologies have shaped recent research in life sciences, enabling researchers to unravel transcriptomic landscapes at the individual cell level and offering unprecedented insights into cellular diversity and functions (1–3). Yet, the requirement for fresh material represents a logistical hurdle, particularly in the context of investigations involving human samples. The inherent challenges associated with the timely collection and processing of such samples have limited the scope of scRNA-seq studies, prompting the exploration of alternative approaches to overcome this constraint.

In respiratory medicine and research, analyses of human bronchoalveolar lavage fluid (BALF) cells are of particular clinical and fundamental utility, both for diagnostic purposes and for understanding disease pathogenesis and treatment responses in the context of lung chronic inflammatory disorders (4–6). The bronchoalveolar lavage procedure allows for the retrieval of cells directly from the airways, offering a unique opportunity to investigate the cellular composition and molecular signatures associated with the healthy and diseased microenvironments. As such, scRNA-seq analyses of BALF cells can provide essential information about the molecular events driving inflammation, immune dysregulation and tissue remodeling in diseased lungs (5–13). They not only enhance our understanding of the cellular dynamics underlying chronic inflammatory conditions, but also paves the way for the identification of potential therapeutic targets and personalized treatment strategies. Arguably, ensuring the preservation of single cell viability and integrity during cryopreservation procedures would allow future translational and clinical investigations in a logistically feasible manner.

AJRCMB Articles in Press. Published May 20, 2025 as 10.1165/rcmb.2024-0467MA

In this study, we compared cryopreservation methods for BALF cells and the subsequent application of droplet-based (10x Chromium) (14) and microwell-based (Honeycomb) scRNA-seq methodologies, and we sought to evaluate the performance of these methods in preserving cellular integrity and transcriptomic signatures of BALF cells, thus providing a valuable resource for the application of scRNA-seq in the field of human respiratory biology.

Methods

Human samples

We analyzed 4 BALF samples collected for routine diagnostic procedures at the pneumology department of the University Hospital (CHU Liège, Belgium). The characteristics of the patients are summarized in Table 1. The use of human BALF cells was approved in 2022 by the Ethics Reviewing Board of the University Hospital of Liege, Belgium (ref. 2022/159).

Reagents and Antibodies

A complete list of the reagents, antibodies and software used in this manuscript can be found in Table E1.

Broncho alveolar lavage fluid (BALF) processing

Human BALFs were processed directly after collection, as explained in the online supplement.

Cytologic examination and differential cell counts of BALF cells

AJRCMB Articles in Press. Published May 20, 2025 as 10.1165/rcmb.2024-0467MA

See online supplement.

BALF cell cryopreservation and droplet-based single cell RNA-sequencing

The technical workflow from sample collection to sequencing is shown in Figure E1. Briefly, after fixation and storage at -80°C, the Chromium Fixed RNA Profiling for Multiplexed Samples method was used following the protocols from 10x Genomics (CG000478 and CG000527). Libraries were sequenced with an estimated sequencing depth of 5 x 10^4 reads per cell. See online supplement for further details.

BALF cell cryopreservation and microwell-based single cell RNA-sequencing

The technical workflow from sample collection to sequencing is shown in Figure E1. Briefly, the HIVE scRNA-seq v1 (Honeycomb Biotechnologies) protocol was used. Libraries were sequenced with an estimated sequencing depth of 5 x 10^4 reads per cell. See online supplement for further details.

Analysis of single cell RNA-sequencing data

Details can be found in the online supplement.

Data and codes availability

The raw fastq files and processed transcript count matrices for this study can be found in the gene expression omnibus database under the accession number GSE276100 (microwell) and GSM8209759 (droplet).

The scripts used to analyse these data have been uploaded to GitHub – https://github.com/JoanAbinet/Micro-Droplet_scRNaseq

AJRCMB Articles in Press. Published May 20, 2025 as 10.1165/rcmb.2024-0467MA

Statistical analysis

Graphs were prepared with GraphPad Prism 10 (GraphPad software) or R Bioconductor. No data were excluded from the analyses. Statistical analyses were performed with Prism 9 (GraphPad software), and with R Bioconductor and Seurat for scRNA-seq data, respectively. The Shapiro-Wilk normality test was employed to assess the distribution of the data. Subsequently, paired tests were conducted, using either the non-parametric Wilcoxon signed-rank test or the non-parametric Kruskal Wallis test, as indicated in the respective figure legends. We considered a *P* value lower than 0.05 to be significant (*, $P < 0.05$; **, $P < 0.01$; ***, $P < 0.001$; ****, $P < 0.0001$; ns, not significant).

Results

Sample processing and experimental pipeline

BALFs were obtained from 4 patients suffering from diverse lung diseases (Table 1). Red blood cells were immunomagnetically depleted directly after collection (Figure E1A). After cell counting, an aliquot of cells was dedicated to cytologic examination and differential cell counting, a second fraction containing 1.5 x 10^4 cells was loaded into one HIVE collector containing microwells with barcoded mRNA-capture beads for entrapment and sequencing (named the “microwell” method hereafter), and the third fraction containing the remaining cells were fixed according to the 10X Genomics protocol and counted for subsequent droplet-based scRNA-seq (named the “droplet” method hereafter) (Figure E1B; Table 2). The HIVE collector and the fixed cells were

AJRCMB Articles in Press. Published May 20, 2025 as 10.1165/rcmb.2024-0467MA

stored at -80°C for a similar period of 2 months for all 4 samples. From this step onwards, the 4 samples were processed in parallel.

The droplet samples were thawed, counted (Table 2) and barcoded before being pooled together and subject to droplet encapsulation using the 10X Genomics platform (14), sequencing and analysis (Figure E1C). Twenty-four hours were needed to process the samples before storage, and 32 hours were needed post-thawing until the sequencing step (Figure E2).

For microwell, the collectors were thawed and sealed, cells were lysed and mRNA was extracted from the collector for cDNA amplification and sequencing (Figure E1C). One hour was needed between sample collection and storage in the collector at -80°C and 8 hours were needed post-thawing until the sequencing step (Figure E1). Of note, the sequencing depth was similar between both techniques and was fixed to 5 x 10^4 reads per cell.

Droplet allows recovery of cells with higher numbers of genes and transcripts compared to microwell

First, we compared the expected *vs.* actual cell recovery rate for each method. Fixed cells for droplet were counted post-thawing and post-hybridization and a volume corresponding to 1.65 x 10^3 cells per sample was loaded into the 10x Genomics platform. Considering an encapsulation rate of 60%, we expected to recover 1 x 10^3 cells per sample (Figure 1A). For microwell, the expected cell recovery for 1.5 x 10^4 loaded cells was 3 x 10^3 cells, as indicated in the manufacturer's procedures (Figure 1A). After sequencing, droplet and microwell data were demultiplexed and a quality control (QC) filtering was applied, with cells with fewer than 400 genes, fewer than 800 unique transcripts and more than 20% mitochondrial genes being removed. The

AJRCMB Articles in Press. Published May 20, 2025 as 10.1165/rcmb.2024-0467MA

threshold of minimum 400 genes was chosen according to the recommendations of Honeycomb. Data from the four droplet samples and data from the four microwell samples were integrated, with integration performed separately for each method to correct for batch effects. A total of 671 +/- 296 (mean +/- SD) cells was recovered for droplet and 935 +/- 807 (mean +/- SD) cells for microwell (Figure 1A), resulting in a higher cell recovery efficiency for droplet (67 %) as compared to microwell (31 %), even though it did not reach statistical significance (P = 0.125) (Figure 1B).

Next, we looked at the number of genes and transcripts detected per cell after QC filtering. An average of 3,107 genes and 13,922 transcripts were detected with droplet, while 1,190 genes and 2,441 transcripts were identified on average with microwell (Table E2). The global distribution and the distribution per human donor (HD) are shown in Figures 1C and 1D and in Figures E3A and E3B, respectively. A significantly higher percentage of mitochondrial genes per cell was detected with microwell (6,23 % [mean]) as compared to droplet (0,58 % [mean]) (Figure 1E; Figure E3C; Table E2). These data show that droplet cells contain higher numbers of genes and transcripts and lower percentage of mitochondrial genes as compared to microwell cells.

Annotation of BALF cell populations analyzed by droplet and microwell

A total of 2,684 and 3,743 cells from all 4 samples passed QC filtering for droplet and microwell, respectively. Graph-based clustering identified 11 and 13 transcriptionally distinct clusters of cells for droplet and microwell, respectively, as visualized on a global Uniform Manifold Approximation and Projection (UMAP) plot (Figures 1F and 1G). UMAP plots of cells segregated by human donors (HD) are shown in Figures E3D and E3E, and the relative contribution of each cluster within each HD sample are shown in Figures 1F and 1G.

AJRCMB Articles in Press. Published May 20, 2025 as 10.1165/rcmb.2024-0467MA

Next, we manually annotated the clusters based on gene expression profiles (Figures 1H and 1I; Figure E4). For droplet, C1-3 expressed high levels of *FABP4*, *MARCO*, *CD68, C1QC* and *MRC1* and were identified as alveolar macrophages (AMs) (Figure 1H). C4 cells expressed high levels of the monocyte-associated genes *CSF1R, VCAN* and *CD14*, high levels of *MAFB* and low levels of the resident AM-related gene *FABP4*, and were thus annotated as *MAFB*+ monocyte-derived macrophages (Mo-Mac) (Figure 1H). C5 was identified as neutrophils (Neu; *CSF3R, S100A8, S100A9*), C6 and C8 as $CD8^+$ T cells (*CD3E, CD8A, GZMB, KLRK1*), C7 as $CD4^+$ T cells (*CD3E, CD4, IL7R*), C9 as cycling T cells (*MKI67*, *TOP2A*, *CD3E*), C10 as mast cells (*KIT, CPA3*) and C11 as epithelial cells (*EPCAM, KRT8, CDH1*) (Figure 1H; Figure E5A-C). Of note, the cell clusters segregated well according to their cell identities of T cells (C6-C9), mononuclear phagocytes (MNPs) and Neu (C1-C5), mast cells (C10) and epithelial cells (C11) on the UMAP plot (Figure 1H).

For microwell, C1-5 were annotated as AMs (Figure 1I). C6 cells were annotated as *MAFB*$^+$ Mo-Macs (*CSF1R, VCAN, CD14*, *MAFB*) and C7 as Neu (*CSF3R, S100A8, S100A9*) (Figure 1I). C8-C10 encompassed T cells based on their expression of *CD4* and/or *CD8*. Of note, the separation between $CD4^+$ and $CD8^+$ T cells was not reflected in distinct clusters, and C10 contained cycling T cells (*MKI67, TOP2A*) (Figure 1I; Figure E5D-F). Interestingly, microwell uniquely allowed the capture of BALF eosinophils (Eos, C11; *SIGLEC8, CCR3, SYNE1*) (Figure 1I; Figures E5G and E5H), despite the fragility and high amounts of RNAses in these cells (15, 16). Finally, C12 and C13 were annotated as epithelial cells (*EPCAM, KRT8, CDH1*) and mast cells (*KIT, CPA3*), respectively (Figure 1I). The proportion of T cells, MNP, Neu, Eos and other cells captured by droplet and microwell are shown in Figures 1J and 1K. Of note, lowering the QC threshold of genes from 400 to 100 genes allowed the recovery of

AJRCMB Articles in Press. Published May 20, 2025 as 10.1165/rcmb.2024-0467MA

4,350 and 7,031 cells for droplet and microwell, respectively, but it was accompanied by the appearance of clusters that could not be annotated and contained very low number of genes (Figures E6A-F and Figure E7; Table E2). Importantly, within the 3,536 and 6,163 annotated cells for droplet and microwell, respectively, the proportions of cell populations were comparable to those observed with the threshold of minimum 400 genes (Figure E6G; Table E2).

Finally, we integrated droplet and microwell datasets together and confirmed that similar cell populations identified either by droplet or microwell clustered well together, at the exception of AMs, in such integrated UMAP (Figure E8). In conclusion, both methods allowed the capture of MNPs, Neu, epithelial cells and mast cells. T cells, known for their low RNA contents (17), seemed to be captured with a higher granularity with droplet, and Eos were uniquely recovered by microwell.

Droplet and microwell have distinct abilities to recover transcripts from BALF cell populations

We performed a manual differential count of BALF cells from cytospins and compared to cell proportions to those obtained by droplet and microwell. In the BALF of HD1, encompassing 67.25% MNPs on the cytospin, the proportions were relatively well reflected in the scRNA-seq data, apart from a relative exhaustion of Neu, especially for microwell (Figure 2A; Table 3). BALF cells of HD2, containing more than 50% T cells on the cytospin, had their relative proportions maintained with droplet, while T cells declined with microwell (Figure 2B; Table 3). The opposite scenario was observed for HD3 BALF cells, containing 47.25% Neu on the cytospin, which were well captured by microwell, while they declined with droplet (Figure 2C; Table 3). In HD4 BALF cells, an enrichment in T cells was observed both with droplet and

AJRCMB Articles in Press. Published May 20, 2025 as 10.1165/rcmb.2024-0467MA

microwell, which was associated with a decrease in the proportion of Neu, especially with droplet (Figure 2D; Table 3). These data show a relatively high variability in the proportions of cells identified by droplet and microwell and support that such proportions do not confidently reflect the cell composition in the initial BALF.

Next, we assessed gene and transcript numbers, as well as the transcript/gene ratio in the different BALF cell populations. We found that droplet largely outperformed microwell for the analysis of AM, epithelial cells and mast cells, based on these 3 parameters (Figures 2E to 2G; Table E2). The performance of droplet was also higher for T cells (Figure 2H; Table E2), while it was comparable for Mo-Mac (Figure 2I; Table E2). Microwell outperformed droplet for the analysis of Neu (Figure 2J; Table E2), and Eos, uniquely detected by microwell, exhibited similar parameters than Neu (Figure 2K; Table E2).

Predictions of transcription factor activities correlate with the numbers of genes and transcripts

Next, we applied single-cell regulatory network inference and clustering (SCENIC) analyses (18) to both droplet and microwell datasets, and heatmaps depicting regulon activities and expression levels of relevant transcriptions factors (TFs) are shown in Figures 3A and 3B, and in Figures E9A and E9B, respectively. First, we observed that expression levels of TFs were very low in a majority of single cells, especially in T cells (Figures E9A and E9B). Second, in the MNP compartment, the AM-imprinting TF PPAR-γ (19) exhibited a high regulon activity in AMs (C1-C3) as compared to other cells from droplet, but was not detected in the 5 clusters of AMs from microwell (Figure 3C). The activity of KLF4, suggested to regulate AMs (20), was higher in AMs as compared to other cells, regardless of the method (Figure 3D). MAFB activity,

AJRCMB Articles in Press. Published May 20, 2025 as 10.1165/rcmb.2024-0467MA

however, was higher in *MAFB*$^{+}$ Mo-Mac (C6) as compared to AMs and other cells from microwell, but had high predicted activities both in AMs and *MAFB*$^{+}$ Mo-Mac (C4) from droplet (Figure 3E). CEBP-δ, a TFs involved in Neu terminal maturation (21, 22), displayed an elevated regulon activity in Neu as compared to other cells, regardless of the scRNA-seq method (Figure 3F). Similarly, T-cell associated TFs, such as TBX21 (23), EOMES (24), GATA3 (25) and MAF (26), had significantly higher activities in T cells from droplet (C6-C9) or microwell (C8-C10) as compared to other cells (Figures 3G to 3J) GATA-2, a TF important for mast cell functional identity (27), was predicted to be active in mast cells from the droplet data (C10), but not detected in mast cells from the microwell data (C13) (Figure 3K). Finally, CEBP-ε, involved in Eos differentiation (16, 28, 29), had its predicted activity higher in Eos (C11) as compared to other cells from microwell (Figure 3L). The data suggest that the number of detected genes and transcripts per cell correlates positively with the probability to infer activities of TFs that are known to play important roles in these cells.

Discussion

In this study, we compared two scRNA-seq methods, droplet-based and microwell-based, for analyzing cryopreserved human BALF cells. Our aim was to determine the efficacy of these methods in preserving cellular integrity and transcriptomic fidelity and our findings provided insights into the strengths and limitations of each approach, contributing to increase our knowledge required to optimize scRNA-seq for cryopreserved human samples.

It is worth emphasizing that distinct methodologies are used to detect genes with the droplet and microwell approaches. Indeed, the droplet-based technology utilizes

AJRCMB Articles in Press. Published May 20, 2025 as 10.1165/rcmb.2024-0467MA

probes designed to target transcripts within the human transcriptome, while the microwell-based technology employs 3' transcript capture oligonucleotides designed to capture the polyadenylated tail of mRNA molecules. Hence, sequencing is performed on probes rather than directly on cDNA with droplet, in contrast to method used with microwell, which sequences the cDNA itself. Of note, while most genes have a three-fold coverage with droplet, some genes are excluded from the probe sets, 7.5% genes have a one-fold coverage, such as those coding for mitochondrial proteins, and 5% genes have more than three probes. As such, the lower percentages of mitochondrial genes observed with droplet, as compared to microwell, might reflect either the one-fold coverage bias for mitochrondrial genes, or improved cell conservation and quality, or a combination of both (30).

Another difference between the two methods was the cell recovery efficiency post-sequencing. Although droplet required a higher initial cell number – the company suggests a minimum of 3 x 10^5 cells for fixation, it ultimately achieved a superior recovery efficiency of intact cells after sequencing and QC filtering when compared to the number of cells loaded into the Chromium. This suggests that, while droplet may have higher upfront demands in terms of biological material, it compensates with better overall efficiency in retaining viable, analyzable cells. That being said, for studies where cell yield can be a major limiting factor, microwell is worth being considered. Indeed, one obvious advantage of microwell is that a few thousand cells are sufficient to be loaded into the collector, despite the lower recovery rate afterwards.

A substantial advantage of droplet was its ability to detect a higher number of genes and transcripts per cell, which was particularly evident for AMs, epithelial cells, mast cells and T cells. In contrast, microwell, while globally less effective in these metrics, uniquely identified fragile eosinophils, highlighting its potential utility in capturing

AJRCMB Articles in Press. Published May 20, 2025 as 10.1165/rcmb.2024-0467MA

specific cell types that might be missed by droplet. Moreover, microwell was equally performant to capture neutrophils. This suggests that microwell may be better suited for certain specialized applications, particularly when dealing with granulocytes, while droplet exhibit a higher performance for the analysis of macrophages, epithelial cells or T cells. Such differences in cell-type capture and transcriptomic profiling underscore the importance of choosing the right method based on the specific research question.

Our analysis of TF activity further demonstrated that droplet generally provided a more detailed and accurate prediction of TF activities for cell populations with the higher number of genes and transcripts detected per cell. Surprisingly, PPAR-γ and GATA-2, major identity-imprinting TF for AMs (19) and mast cells (27), respectively, were not predicted in AMs and mast cells from microwell. However, CEBP-δ, a TF important in neutrophil terminal maturation (21, 22), was predicted in both datasets, correlating with similar numbers of genes and transcripts detected in neutrophils from droplet and microwell. Similarly, CEBP-ε was accurately predicted in Eos (16, 28, 29), which were uniquely captured by microwell, which could be leveraged in studies investigating eosinophil-associated disorders. Surprisingly, the inferred activities of MAFB displayed discrepant results between droplet and microwell methods. While both approaches identified high MAFB activity in Mo-Macs, as expected (30, 31), droplet also predicted an elevated MAFB regulatory potential in AMs, which is not in line with findings supporting that resident AMs are not dependent on MAFB (31–33). If the AMs analyzed in these BALFs are no longer embryonically-derived but have been replenished by monocytes in adults and therefore exhibit high MAFB activity (34), this phenomenon should also be reflected in the microwell data. Alternatively, the discrepancy might stem from a 'non-biological' factor, such as technical artifacts or method-specific biases.

AJRCMB Articles in Press. Published May 20, 2025 as 10.1165/rcmb.2024-0467MA

A limitation of our study is its focus on BALF cells collected from patients suffering from diverse pulmonary conditions, which necessitates caution when generalizing our conclusions to other diseases, tissues, or cellular contexts. While we observed performance differences between droplet and microwell methods, it remains uncertain whether similar results would be obtained with blood cells or those derived from enzymatically digested tissues. Cells originating from blood, being more robust and less sensitive to processing, might minimize differences in cell recovery and transcriptomic profiling between the two methods. Conversely, enzymatically digested tissues, which often rely heavily on digestion protocols and contain fragile epithelial cells, may exhibit greater variability in performance metrics. Another factor to consider is that our findings were derived from BALF samples obtained in the context of inflammatory conditions, where specific immune cell populations, such as eosinophils or neutrophils, might be more prevalent and activated. It is possible that BALF cells collected during non-inflammatory conditions, where immune cell diversity and activation states are likely distinct, may yield different performance metrics for each method. Future studies comparing these methods across diverse sample types and physiological conditions will be crucial to establish the generalizability of our findings and expand their applicability to broader biological and clinical contexts.

In conclusion, our comparative analysis revealed that the droplet-based method generally outperforms the microwell-based method in terms of cell recovery efficiency, transcriptomic abundance, and TF activity prediction. However, the microwell method’s unique ability to capture fragile cell types like Eos suggests that it has a niche utility. Researchers should consider these trade-offs when designing scRNA-seq studies, especially in the context of cryopreserved human samples where cell viability and integrity are paramount. Our findings provided a valuable resource for the

AJRCMB Articles in Press. Published May 20, 2025 as 10.1165/rcmb.2024-0467MA

design of future large-scale translational and clinical projects utilizing scRNA-seq, particularly in the field of respiratory medicine.

Ackowledgements

The authors thank all members of the Immunophysiology laboratory (GIGA Institute, University of Liège, Belgium), of the laboratory of Pneumology (GIGA Institute, University of Liège, Belgium), of the pneumology department (CHU Liège, Belgium), and Pauline Maréchal, Monica Di Cesare, Cédric François, Raja Fares, and Ilham Sbai for their excellent technical and administrative support.

Thomas Marichal acknowledges support from the F.R.S.-FNRS (Incentive Grant for Scientific Research), from the FRFS-Welbio, from the Acteria Foundation and from an ERC Starting Grant (ERC StG 2018 IM-ID: 801823). Thomas Marichal is supported by a Research Project Grant of the F.R.S.-FNRS, by a FRFS-Welbio Advanced Grant (WELBIO-CR-2022A-10), by an ERC Consolidator Grant (ERC CoG 2023 MoMacTrajectALI: 101124390), by the Baillet Latour Fund and by the Léon Fredericq Foundation. Coraline Radermecker is a Research Associate of the F.R.S.-FNRS.

AJRCMB Articles in Press. Published May 20, 2025 as 10.1165/rcmb.2024-0467MA

References

1. Jaitin DA, Kenigsberg E, Keren-Shaul H, Elefant N, Paul F, Zaretsky I, *et al.* Massively parallel single-cell RNA-seq for marker-free decomposition of tissues into cell types. *Science* 2014;343:776–779.
2. Ding J, Adiconis X, Simmons SK, Kowalczyk MS, Hession CC, Marjanovic ND, *et al.* Systematic comparison of single-cell and single-nucleus RNA-sequencing methods. *Nat Biotechnol* 2020;38:737–746.
3. Ginhoux F, Yalin A, Dutertre CA, Amit I. Single-cell immunology: Past, present, and future. *Immunity* 2022;55:393–404.
4. Davidson KR, Ha DM, Schwarz MI, Chan ED. Bronchoalveolar lavage as a diagnostic procedure: a review of known cellular and molecular findings in various lung diseases. *J Thorac Dis* 2020;12:4991–5019.
5. Karmaus PWF, Tata A, Meacham JM, Day F, Thrower D, Tata PR, *et al.* Meta-Analysis of COVID-19 BAL Single-Cell RNA Sequencing Reveals Alveolar Epithelial Transitions and Unique Alveolar Epithelial Cell Fates. *Am J Respir Cell Mol Biol* 69:623–637.
6. Alladina J, Smith NP, Kooistra T, Slowikowski K, Kernin IJ, Deguine J, *et al.* A human model of asthma exacerbation reveals transcriptional programs and cell circuits specific to allergic asthma. *Sci Immunol* 2023;8:eabq6352.
7. Liao M, Liu Y, Yuan J, Wen Y, Xu G, Zhao J, *et al.* Single-cell landscape of bronchoalveolar immune cells in patients with COVID-19. *Nat Med* 2020;26:842–844.
8. Liégeois M, Bai Q, Fievez L, Pirottin D, Legrand C, Guiot J, *et al.* Airway Macrophages Encompass Transcriptionally and Functionally Distinct Subsets Altered by Smoking. *Am J Respir Cell Mol Biol* 2022;67:241–252.

AJRCMB Articles in Press. Published May 20, 2025 as 10.1165/rcmb.2024-0467MA

9. Moshkelgosha S, Duong A, Wilson G, Andrews T, Berra G, Renaud-Picard B, *et al.* Interferon-stimulated and metallothionein-expressing macrophages are associated with acute and chronic allograft dysfunction after lung transplantation. *J Heart Lung Transplant Off Publ Int Soc Heart Transplant* 2022;41:1556–1569.

10. Li H, Wang H, Sokulsky L, Liu S, Yang R, Liu X, *et al.* Single-cell transcriptomic analysis reveals key immune cell phenotypes in the lungs of patients with asthma exacerbation. *J Allergy Clin Immunol* 2021;147:941–954.

11. Mould KJ, Moore CM, McManus SA, McCubbrey AL, McClendon JD, Griesmer CL, *et al.* Airspace Macrophages and Monocytes Exist in Transcriptionally Distinct Subsets in Healthy Adults. *Am J Respir Crit Care Med* 2021;203:946–956.

12. Sauler M, McDonough JE, Adams TS, Kothapalli N, Barnthaler T, Werder RB, *et al.* Characterization of the COPD alveolar niche using single-cell RNA sequencing. *Nat Commun* 2022;13:494.

13. Fastrès A, Pirottin D, Fievez L, Tutunaru A-C, Bolen G, Merveille A-C, *et al.* Identification of Pro-Fibrotic Macrophage Populations by Single-Cell Transcriptomic Analysis in West Highland White Terriers Affected With Canine Idiopathic Pulmonary Fibrosis. *Front Immunol* 2020;11:611749.

14. Zheng GX, Terry JM, Belgrader P, Ryvkin P, Bent ZW, Wilson R, *et al.* Massively parallel digital transcriptional profiling of single cells. *Nat Commun* 2017;8:14049.

15. Wilkerson EM, Johansson MW, Hebert AS, Westphall MS, Mathur SK, Jarjour NN, *et al.* The Peripheral Blood Eosinophil Proteome. *J Proteome Res* 2016;15:1524–1533.

AJRCMB Articles in Press. Published May 20, 2025 as 10.1165/rcmb.2024-0467MA

16. Jorssen J, Van Hulst G, Mollers K, Pujol J, Petrellis G, Baptista AP, *et al.* Single-cell proteomics and transcriptomics capture eosinophil development and identify the role of IL-5 in their lineage transit amplification. *Immunity* 2024;57:1549-1566.e8.

17. Wang J, Rieder SA, Wu J, Hayes S, Halpin RA, de Los Reyes M, *et al.* Evaluation of ultra-low input RNA sequencing for the study of human T cell transcriptome. *Sci Rep* 2019;9:8445.

18. Aibar S, González-Blas CB, Moerman T, Huynh-Thu VA, Imrichova H, Hulselmans G, *et al.* SCENIC: single-cell regulatory network inference and clustering. *Nat Methods* 2017;14:1083–1086.

19. Schneider C, Nobs SP, Kurrer M, Rehrauer H, Thiele C, Kopf M. Induction of the nuclear receptor PPAR-gamma by the cytokine GM-CSF is critical for the differentiation of fetal monocytes into alveolar macrophages. *Nat Immunol* 2014;15:1026–37.

20. Pestal K, Slayden LC, Barton GM. Krüppel-like Factor (KLF) family members control expression of genes required for serous cavity and alveolar macrophage identities. *BioRxiv Prepr Serv Biol* 2024;2024.02.28.582578.doi:10.1101/2024.02.28.582578.

21. Jauch-Speer S-L, Herrera-Rivero M, Ludwig N, Véras De Carvalho BC, Martens L, Wolf J, *et al.* C/EBPδ-induced epigenetic changes control the dynamic gene transcription of S100a8 and S100a9. *eLife* 2022;11:e75594.

22. Evrard M, Kwok IWH, Chong SZ, Teng KWW, Becht E, Chen J, *et al.* Developmental Analysis of Bone Marrow Neutrophils Reveals Populations Specialized in Expansion, Trafficking, and Effector Functions. *Immunity* 2018;48:364-379 e8.

AJRCMB Articles in Press. Published May 20, 2025 as 10.1165/rcmb.2024-0467MA

23. Mohamed R, Lord GM. T-bet as a key regulator of mucosal immunity. *Immunology* 2016;147:367–376.

24. Dejean AS, Joulia E, Walzer T. The role of Eomes in human CD4 T cell differentiation: A question of context. *Eur J Immunol* 2019;49:38–41.

25. Zhou M, Ouyang W. The function role of GATA-3 in Th1 and Th2 differentiation. *Immunol Res* 2003;28:25–37.

26. Imbratta C, Hussein H, Andris F, Verdeil G. c-MAF, a Swiss Army Knife for Tolerance in Lymphocytes. *Front Immunol* 2020;11:206.

27. Li Y, Gao J, Kamran M, Harmacek L, Danhorn T, Leach SM, *et al.* GATA2 regulates mast cell identity and responsiveness to antigenic stimulation by promoting chromatin remodeling at super-enhancers. *Nat Commun* 2021;12:494.

28. Shyamsunder P, Shanmugasundaram M, Mayakonda A, Dakle P, Teoh WW, Han L, *et al.* Identification of a novel enhancer of CEBPE essential for granulocytic differentiation. *Blood* 2019;133:2507–2517.

29. Ben-Baruch Morgenstern N, Rochman M, Kotliar M, Dunn JLM, Mack L, Besse J, *et al.* Single-cell RNA-sequencing of human eosinophils in allergic inflammation in the esophagus. *J Allergy Clin Immunol* 2024;S0091-6749(24)00602-X.doi:10.1016/j.jaci.2024.05.029.

30. Ruscitti C, Abinet J, Maréchal P, Meunier M, de Meeûs C, Vanneste D, *et al.* Recruited atypical Ly6G+ macrophages license alveolar regeneration after lung injury. *Sci Immunol* 2024;9:eado1227.

31. Vanneste D, Bai Q, Hasan S, Peng W, Pirottin D, Schyns J, *et al.* MafB-restricted local monocyte proliferation precedes lung interstitial macrophage differentiation. *Nat Immunol* 2023;24:827–840.

AJRCMB Articles in Press. Published May 20, 2025 as 10.1165/rcmb.2024-0467MA

32. Aziz A, Soucie E, Sarrazin S, Sieweke MH. MafB/c-Maf deficiency enables self-renewal of differentiated functional macrophages. *Science* 2009;326:867–71.

33. Molawi K, Sieweke MH. Transcriptional control of macrophage identity, self-renewal, and function. *Adv Immunol* 2013;120:269–300.

34. Kelly LM, Englmeier U, Lafon I, Sieweke MH, Graf T. MafB is an inducer of monocytic differentiation. *EMBO J* 2000;19:1987–1997.

AJRCMB Articles in Press. Published May 20, 2025 as 10.1165/rcmb.2024-0467MA

Tables

Table 1. Characteristics of human patients from which originate the BALF cells analyzed by single cell RNA-sequencing. HD, human donor; F, female; M, male; yr, years; nsp., nonspecific; CMV, cytomegalovirus

HD	**1**	**2**	**3**	**4**
Gender	F	M	M	M
Age (yr)	63	58	71	71
Know co-morbidities	Immunosuppressed, kidney transplant	Interstitial pneumonia with auto-immune features (IPAF)	Lung fibrosis	Immunosuppressed, interstitial pneumonia with anti-synthetase syndrome (SAS)
Secondary lung infection	Bronchopneumonia *nsp.*	Metapneumovirus & CMV infections	Bronchopneumonia *Klebsiella oxytaca*	Bronchopneumonia *nsp.*

AJRCMB Articles in Press. Published May 20, 2025 as 10.1165/rcmb.2024-0467MA

Table 2. Number of fresh cells dedicated to cytospin, droplet and microwell, of recovered cells for droplet post-fixation, and of cells analyzed by each scRNA_seq method post-QC and filtering.

	Cell Number (fresh)			Cell Number (post-fixation)		Cell Number (post-QC and filtering)	
	Cytospin	Droplet	Microwell	Droplet	Microwell	Droplet	Microwell
HD 1	96 $x10^3$	2,4 $x10^6$	1,5 $x10^4$	1,02 $x10^6$	/	971	1,841
HD 2	32 $x10^3$	8 $x10^5$	1,5 $x10^4$	2,4 $x10^5$	/	834	248
HD 3	8 $x10^3$	2 $x10^5$	1,5 $x10^4$	1 $x10^5$	/	301	262
HD 4	228 $x10^3$	5,7 $x10^6$	1,5 $x10^4$	2,22 $x10^6$	/	578	1,392

AJRCMB Articles in Press. Published May 20, 2025 as 10.1165/rcmb.2024-0467MA

Table 3. Percentages of cell populations obtained by droplet and microwell compared to the differential cell count of BALF cells.

		MNP	T cell	Eos	Neu	Other cells
HD 1	Cytospin	67.25	2.25	0.25	30	0.25
	Droplet	68.90	5.46	0.00	20.39	5.25
	Microwell	92.02	1.63	0.00	5.05	1.3
HD 2	Cytospin	23.67	57.00	4.00	13.33	2.00
	Droplet	31.77	52.52	0.00	6.12	9.59
	Microwell	47.58	28.63	2.82	6.45	14.52
HD 3	Cytospin	7.50	20.50	23.25	47.25	1.50
	Droplet	5.98	71.76	0.00	15.61	6.64
	Microwell	12.21	21.76	16.79	46.56	2.67
HD 4	Cytospin	32.80	32.60	5.40	29.20	0.00
	Droplet	20.93	76.99	0.00	0.17	1.90
	Microwell	8.33	80.24	0.50	10.56	0.36

AJRCMB Articles in Press. Published May 20, 2025 as 10.1165/rcmb.2024-0467MA

Figure Legends

Figure 1. Comparison of droplet and microwell methods in terms of cell recovery efficiency, gene and transcript numbers, single cell identities and frequencies of human BALF cells. *(A)* Bar graph showing the expected vs. actual cell number recovered post-QC assessment with each method. *(B)* Bar graph showing cell recovery efficiency compared to the expected 100% efficiency with each method. *(C)* Violin plot (height: gene number; width: abundance or cells) depicting the number of genes detected in single cells with both methods. *(D)* Violin plot (height: transcript number; width: abundance or cells) depicting the number of transcripts detected in single cells with both methods, as in (C). *(E)* Violin plot (height: % of mitochondrial genes; width: abundance or cells) depicting the % of mitochondrial genes detected in single cells with both methods, as in (C). *(F)* Uniform Manifold Approximation and Projection (UMAP) plots of droplet scRNA-seq data depicting the transcriptional identity of human BALF cells. The frequency of each annotated cluster is shown on the right. (*G*) UMAP plots of microwell scRNA-seq data depicting the transcriptional identity of human BALF cells. The frequency of each annotated cluster is shown on the right. *(H,I)* Dot plots displaying the average expression of the indicated genes and the percentage of cells expressing those genes within each cluster analyzed by droplet (*H*) and microwell *(I)*. *(J,K)* Pie charts showing the frequency of the indicated cell populations analyzed by droplet (*J*) or microwell (*K*) across the merged data from 4 HD. (A,B) Data show mean ± SEM as well as individual values. (*B,C,D,E*) *P* values were calculated using a non-parametric paired Wilcoxon signed-rank test. ****, $P < 0.0001$. AM, Alveolar Macrophage; Eos, Eosinophil; Mo-Mac, monocyte-derived macrophage; Neu, Neutrophil.

AJRCMB Articles in Press. Published May 20, 2025 as 10.1165/rcmb.2024-0467MA

Figure 2. Performance of droplet and microwell in recovering and capturing distinct BALF cell populations. (*A-D*) Pie charts showing the proportions of the indicated cell populations determined by morphological assessment of cytospin slides from fresh samples compared to those determined by droplet and microwell, for human donor (HD) 1 (*A*), HD2 (*B*), HD3 (*C*) and HD4 (*D*). *(E-K)* Violin plot (height: gene number, transcript number or transcript / gene ratio; width: abundance of cells) comparing the number of genes, number of transcripts or the transcript/gene ratio in droplet vs. microwell AMs (*E*), epithelial cells (*F*), mast cells (*G*), T cells (*H*), Mo-Mac (*I*), neutrophils (*J*) and eosinophils (*K*). (*E-J) P* values were calculated using a non-parametric paired Wilcoxon signed-rank test. ****, $P < 0.0001$. AM, Alveolar Macrophage; Eos, Eosinophil; Mo-Mac, monocyte-derived macrophage; Neu, Neutrophil.

Figure 3. Inference of transcription factor activities in BALF cells analyzed by droplet and microwell. (*A,B*) Heatmap depicting predicted activities of the indicated transcription factors (TFs) across human BALF cells, evaluated by SCENIC analysis of the droplet (*A*) and microwell (*B*) scRNA-seq data. *(C-L)* Violin plots (height: regulon activity; width: abundance of cells) depicting the transcription factor activities of PPAR-γ (*C*), KLF4 (*D)*, MAFB (*E*), CEBP-δ (*F*), TBX21 (*G*), EOMES (*H*), GATA3 (*I*), MAF (*J*), GATA2 (*K*) and CEBP-ε (*L*) predicted in the indicated cell populations analyzed by either droplet or microwell. *P* values were calculated a non-parametric Kruskal-Wallis signed-rank test. ****, $P < 0.0001$.

AJRCMB Articles in Press. Published May 20, 2025 as 10.1165/rcmb.2024-0467MA

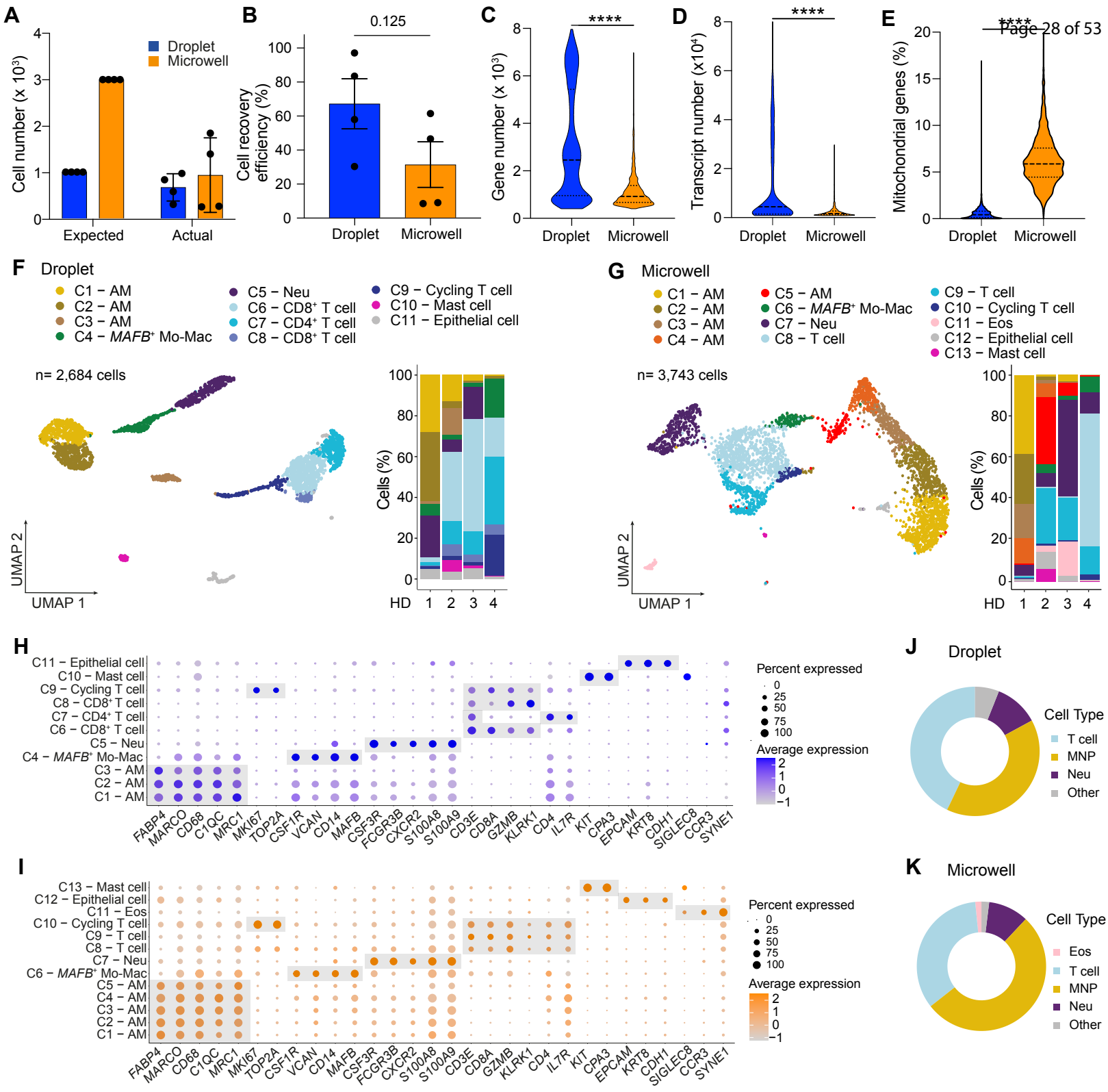

Figure 1

AJRCMB Articles in Press. Published May 20, 2025 as 10.1165/rcmb.2024-0467MA

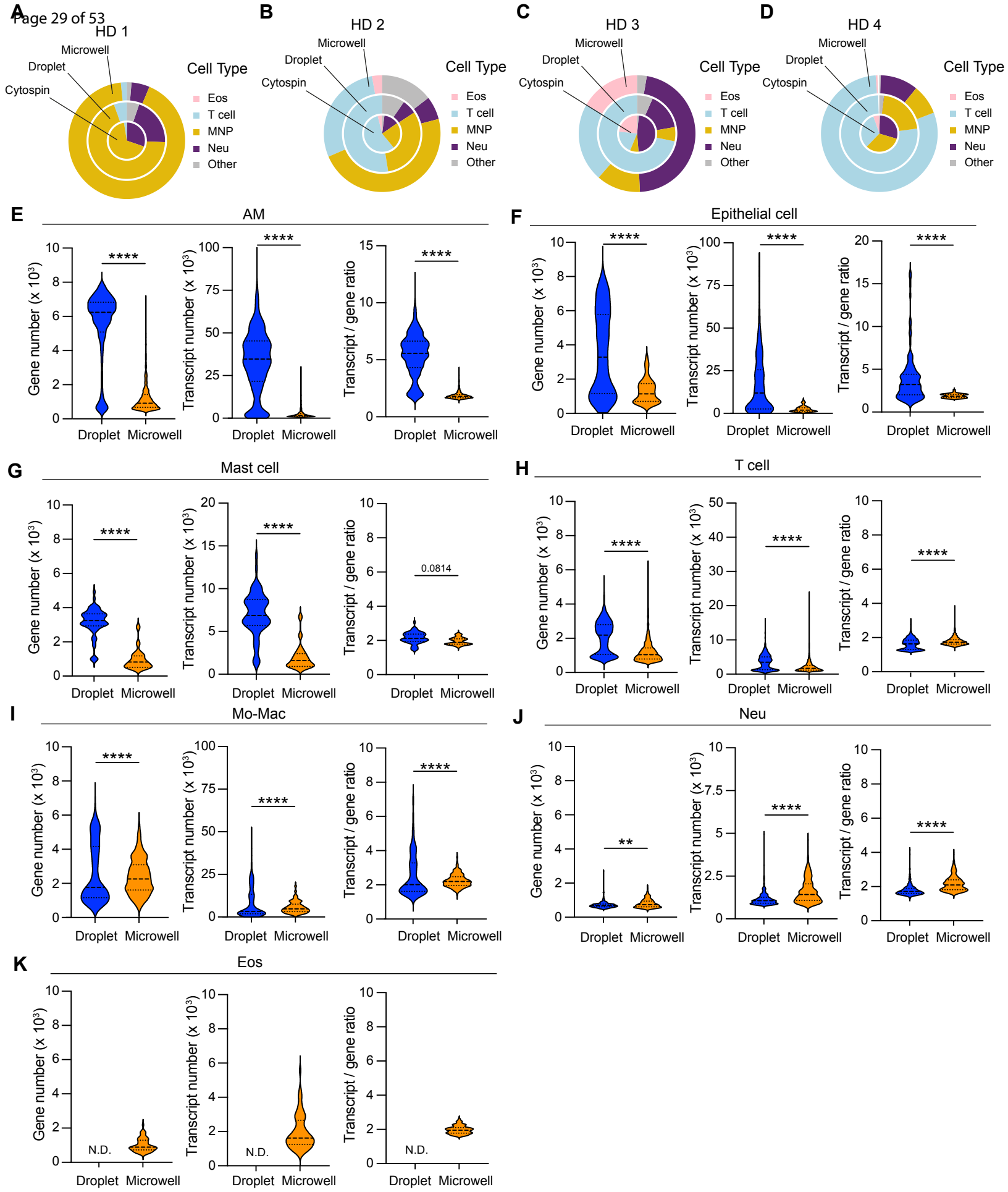

Figure 2

AJRCMB Articles in Press. Published May 20, 2025 as 10.1165/rcmb.2024-0467MA

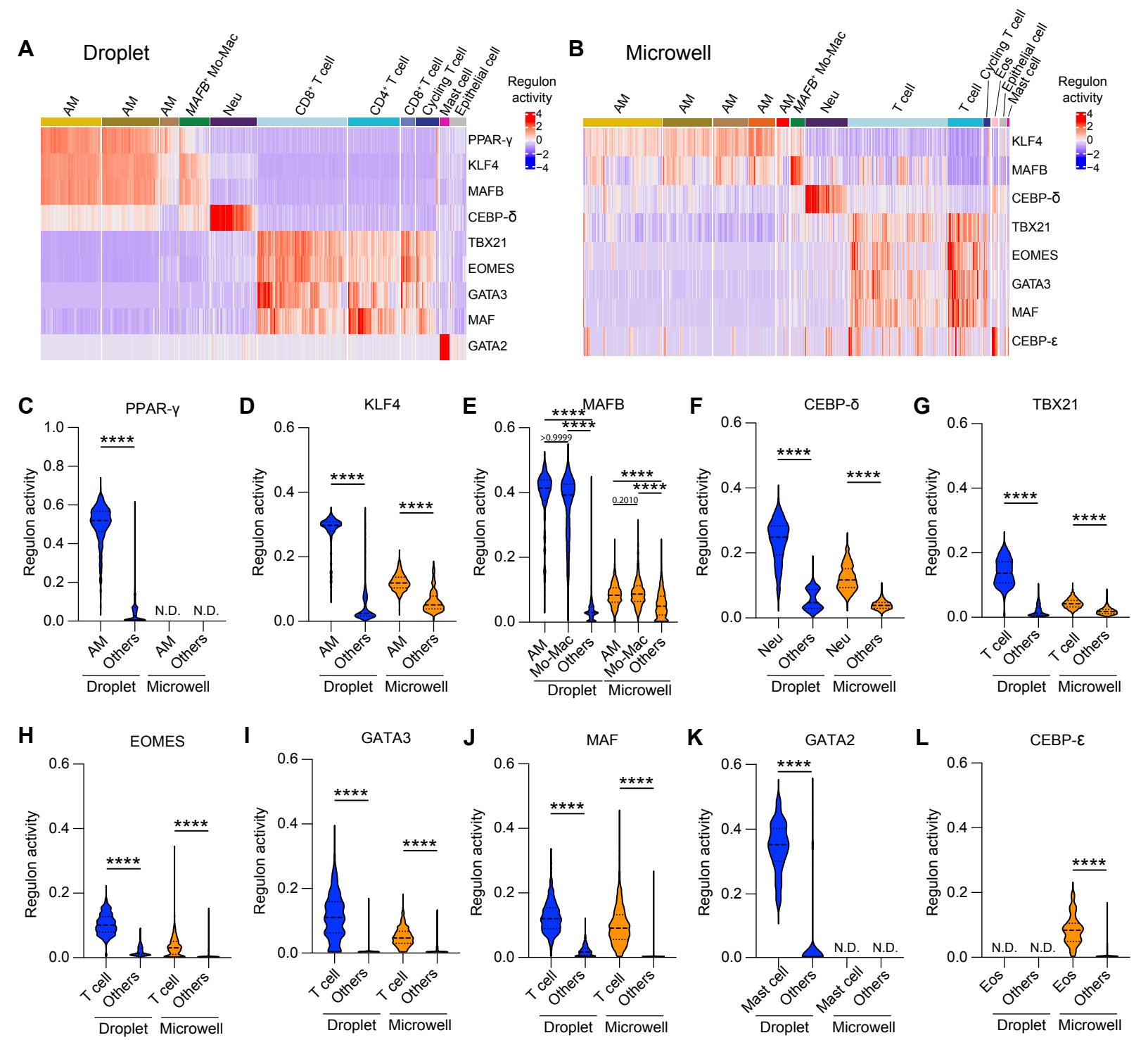
A
Droplet
AM
AM
AM
MAFB+ Mo-Mac
Neu
CD8+ T cell
CD4+ T cell
CD8+ T cell
Cycling T cell
Mast cell
Epithelial cell
Regulon activity
4
2
0
−2
−4
PPAR-γ
KLF4
MAFB
CEBP-δ
TBX21
EOMES
GATA3
MAF
GATA2
B
Microwell
AM
AM
AM
AM
AM
MAFB+ Mo-Mac
Neu
T cell
T cell
Cycling T cell
Eos
Epithelial cell
Mast cell
Regulon activity
4
2
0
−2
−4
KLF4
MAFB
CEBP-δ
TBX21
EOMES
GATA3
MAF
CEBP-ε
C
PPAR-γ
Regulon activity
1.0
0.8
0.6
0.4
0.2
0.0
****
N.D.
N.D.
AM
Others
AM
Others
Droplet
Microwell
D
KLF4
Regulon activity
0.6
0.4
0.2
0.0
****
****
AM
Others
AM
Others
Droplet
Microwell
E
MAFB
Regulon activity
0.6
0.4
0.2
0.0
****
****
>0.9999
****
****
0.2010
AM
Mo-Mac
Others
AM
Mo-Mac
Others
Droplet
Microwell
F
CEBP-δ
Regulon activity
0.6
0.4
0.2
0.0
****
****
Neu
Others
Neu
Others
Droplet
Microwell
G
TBX21
Regulon activity
0.6
0.4
0.2
0.0
****
****
T cell
Others
T cell
Others
Droplet
Microwell
H
EOMES
Regulon activity
0.6
0.4
0.2
0.0
****
****
T cell
Others
T cell
Others
Droplet
Microwell
I
GATA3
Regulon activity
0.6
0.4
0.2
0.0
****
****
T cell
Others
T cell
Others
Droplet
Microwell
J
MAF
Regulon activity
0.6
0.4
0.2
0.0
****
****
T cell
Others
T cell
Others
Droplet
Microwell
K
GATA2
Regulon activity
0.6
0.4
0.2
0.0
****
N.D.
N.D.
Mast cell
Others
Mast cell
Others
Droplet
Microwell
L
CEBP-ε
Regulon activity
0.6
0.4
0.2
0.0
N.D.
N.D.
****
Eos
Others
Eos
Others
Droplet
Microwell

Comparison of Droplet- and Microwell-based Methods to Analyze Cryopreserved Human Bronchoalveolar Lavage Cells by scRNA-Sequencing

Pierre Janssen, DVM, Joan Abinet, MSc, Latifa Karim, Wouter Coppieters, PhD, Catherine Moermans, DVM, PhD, Julien Guiot, MD, PhD, Florence Schleich, MD, PhD, Coraline Radermecker, DVM, PhD & Thomas Marichal, DVM, PhD

ONLINE DATA SUPPLEMENT

AJRCMB Articles in Press. Published May 20, 2025 as 10.1165/rcmb.2024-0467MA

Supplemental Material and Methods

Broncho alveolar lavage fluid (BALF) processing

Human BALFs were processed directly after collection. The different collection tubes were pooled together per patient and were centrifuged (1400 rpm or 414 x *g*, 7 min, rotor S-4-104 Centrifuge 5810R, Eppendorf). Cell pellets were resuspended in 1 mL of PBS containing 6 mM EDTA (1084181000, Merck Millipore) and 2% Fetal Bovine Serum (FBS) (F7524, Sigma). Following the passage of the endoscope through the respiratory tract, minor bleeding may occur. Potentially contaminating red blood cells were eliminated using the EasySep™ RBC Depletion Kit (18170, STEMCELL Technologies Inc.). Briefly, 50 µL of RBC reagent were added and the suspension was incubated for 5 minutes into the EasySep™ magnet (18000, STEMCELL Technologies Inc.). The BALF cell suspension was poured into another 5 mL polypropylene tube and the procedure was repeated three times. For viable cell counting, we performed a staining with Trypan Blue (15250061, Thermofisher) and counted using a Thoma cell chamber.

After counting, an aliquot of cells (fraction 1) was dedicated to cytologic examination and differential cell counting (see below) and we separated samples in two fractions: one fraction (fraction 2) with 1,5 x 10^4 cells per sample for microwell-based scRNA-seq (see below), and another fraction (fraction 3) containing the remaining cells for droplet-based scRNA-seq (Table 2).

Cytologic examination and differential cell counts of BALF cells

Immediately after RBC depletion, 40 µL from a total volume of 1 mL of fresh BALF was diluted in 160 µL PBS (i.e., fraction 1). The resulting cell suspension was

AJRCMB Articles in Press. Published May 20, 2025 as 10.1165/rcmb.2024-0467MA

subsequently centrifuged (1000 rpm or 112 x *g*, 4 minutes, rotor JC 301 Cellspin I 1206-14, Tharmac) and spread on a cytospin slide. The 4 slides were then stained with May-Grünwald-Giemsa (MGG). Differential cell counts, including macrophages, lymphocytes, neutrophils, eosinophils, and epithelial cells, were conducted by examining a minimum of 400 cells through a standard light microscope at 40x magnification. The proportion of each cell type was calculated as a percentage of the total cell population.

BALF cell cryopreservation and droplet-based single cell RNA-sequencing

The technical workflow from sample collection to sequencing is shown in Figure E1. Fresh BALF cells of fraction 3 underwent centrifugation at 400 x *g* for 5 minutes at room temperature. For fixation, we adapted the protocol CG000478 (10x Genomics). Briefly, 1 mL of buffer was prepared by combining 100 µL of Concentrated Fix & Perm Buffer (PN-2000517, 10x Genomics) with 108.1 µL of formaldehyde 37% (10532955, Fisher) and 791.9 µL nuclease-free water for each BALF cell sample. The resulting solution was then incubated at 4°C for 24 hours. After a subsequent 5 minutes centrifugation at 850 x *g* and removal of the supernatant, fixed cells were mixed with 1 mL of Quenching Buffer. The Quenching Buffer consisted of 125 µL of Concentrated Quench Buffer (PN-2000516, 10x Genomics) and 875 µL nuclease-free water, and this mixture was placed in DNA LoBind tubes (1.5 mL, 022431021, Eppendorf). Post-fixation, cells post fixation were then counted using 20 µL of cell suspension and 20 µL of staining solution, comprising 12 µM 4',6-diamidino-2-phenylindole (DAPI) (D3571, ThermoFisher) and 12 µM propidium iodide (PI) (ENZ-52403, Enzo life sciences) in nuclease-free water. Immunofluorescence counting was performed using an Echo Revolution fluorescent microscope (Echo, San Diego, CA, USA) after loading

AJRCMB Articles in Press. Published May 20, 2025 as 10.1165/rcmb.2024-0467MA

the fixed cells into a Thoma cell counting chamber (Table 2). Following the counting step, 100 µL of pre-warmed Enhancer (PN-2000482, 10x Genomics) was added to the Quenching Buffer-fixed sample. Subsequently, 275 µL of 50% glycerol (327255000, Sigma) was finally added to the mixture. The DNA LoBind tubes containing the fixed sample were then stored at -80 °C for a similar period of 2 months for all 4 samples.

The Chromium Fixed RNA Profiling for Multiplexed Samples method was used following the protocols from 10x Genomics (CG000478 and CG000527). This approach enables the storage of fixed cells and facilitates the analysis of multiple samples in a single Gel Bead-in-Emulsion (GEM) reaction. After storing 4 samples at -80°C for 2 months, post storage processing consisted in extracting cryovials containing fixed cells and allowing them to thaw at room temperature and centrifugate them at 850 x *g* for 5 minutes. Subsequently, the supernatant was removed and the thawed cells were washed by adding 1 mL 0.5 X PBS containing 0.02 % UltraPure Bovine Serum Albumin (BSA) (AM2616, ThermoFisher Scientific) and counted with Countess™3 Automated Cell Counter (AMQAX2000, ThermoFisher Scientific). Cells were centrifuged and resuspended in hybridization buffer. For probe hydridization, the Chromium Next GEM Single Cell Fixed RNA Human Transcriptome Probe Kit (PN-1000420, 10X Genomics) was used. Each fixed single-cell suspension was mixed with a different barcoded probe-set and a hybridization mix buffer for 20 hours in a thermal cycler Veriti™ (4375305, ThermoFisher) at 42°C. After hybridization, cells were diluted in a Post Hyb wash buffer and counted with Countess™3 Automated Cell Counter (AMQAX2000, ThermoFisher Scientific). Samples were pooled equally using a worksheet (Document GC000565, 10x Genomics). All washing steps were done on the pooled cells accordingly to 10x Genomics Protocol. After the last step of washing,

AJRCMB Articles in Press. Published May 20, 2025 as 10.1165/rcmb.2024-0467MA

pooled cells were filtered through a 30 µm filter (130-041-407, Miltenyi Biotec) and counted again (Countess™3). A total of 6.6 x 10^3 cells (1.65 x 10^3 cells from each sample) were loaded into the Chromium iX - Next GEM Chip Q (PN-2000518, 10x Genomics). The cells were then partitioned, and their probes were captured and barcoded using Single Cell TL v1 Gel Bead (PN-2000538, 10x Genomics). After droplet generation, the partitioned cells, Gel Beads, and Master Mix were slowly transferred (100 µL) in a strip of 8 tubes (lo bind, Bioke), and incubated overnight in a thermal cycler Veriti™ (4375305, ThermoFisher). During incubation, a ligation step occurred to seal left hand and right hand probe while the probes remain hybridized to their target RNA target, followed by hybridization of the Gel Beads primer to capture sequence on the ligated probe pair. A polymerase then extended this to add the UMI, 10x GEM Barcode, and Read 1T. Enzymes in the GEM reaction were inactivated by heat denaturation. After ligation and barcoding, the GEMs were broken using Recovery Agent (PN-220016, 10x Genomics). The ligated product was pre-amplified for 8 cycles using a PCR master mix and then purified with SPRIselect reagent kit (B23318, Beckman Coulter). Only 1/5 th of Preamplified product were used for Dual Indexing PCR for a total of 15 cycles. QIAxel (QIAGEN) was used to determine the size, library profile and the molarity was calculated based on qPCR data (KAPA Library Quantification KIT, KAPA Biosystems). The final library, prepared for sequencing, was a standard Illumina paired-end constructs which P5 and P7 adaptors. Sequencing was conducted on a NovaSeq™ 6000 sequencer (Illumina) on a S4 flow cell (Rd1: 28 cycles; i1: 10 cycles; i2: 10 cycles; Rd2: 90 cycles) with an estimated sequencing depth of 5 x 10^4 reads per cell.

BALF cell cryopreservation and microwell-based single cell RNA-sequencing

AJRCMB Articles in Press. Published May 20, 2025 as 10.1165/rcmb.2024-0467MA

The technical workflow from sample collection to sequencing is shown in Figure E1. Fresh BALF cells from fraction 2 containing were prepared with Cell Preservation Solution (Honeycomb Biotechnologies) and loaded into one HIVE Collector (Honeycomb Biotechnologies) per donor, following the manufacturer's instructions (v1 revision A). Each HIVE Collector contains over 65 x 10^3 picowells preloaded with barcoded 3’ transcript capture beads. The collectors were stored at - 80 °C for 2 months, allowing the simultaneous processing and sequencing of fo4ur collectors. Before sequencing, the HIVE Collectors were thawed at room temperature for 60 minutes. The Cell Preservation Solution was removed, and the cells were washed with the appropriate Wash Solution (Honeycomb Biotechnologies). The Cell Loader was then replaced with the HIVE Top (Honeycomb Biotechnologies), and the system was incubated at 50°C for 30 minutes. Following this, cells were lysed, and hybridization was performed at room temperature for 30 minutes. After removing the Hybridization Solution, Bead Recovery Solution (Honeycomb Biotechnologies) was added through the covered port of the collectors, and the Cell Loader was centrifuged to collect the bead pellet. The bead pellet was transferred to a filter plate. The recovered beads were transferred onto a filter plate. First-strand synthesis and second-strand synthesis were processed on the filter plate and in a cycler. Between each reaction, a wash was performed using a vacuum system. For the next step of whole-genome amplification, the beads (Honeycomb Biotechnologies) were resuspended in PCR mix, and amplification was carried out on a PCR plate, followed by a SPRI cleanup. The library preparation was completed with an 8-cycles indexing PCR (a different index for each sample), followed by a SPRI cleanup. Final library concentrations were measured using a KAPA Library Quantification KIT (KAPA Biosystems) and quality check was done on Bioanalyzer with HS DNA kit (Agilent). The molarity of each library was

AJRCMB Articles in Press. Published May 20, 2025 as 10.1165/rcmb.2024-0467MA

calculated based on Bioanalyzer and qPCR data (Sigma). Sequencing was performed on a NextSeq™ 550 sequencer (Illumina) using an NextSeq550 V2.5 75-cycles high mode flow cell (Rd1: 25 cycles; i1: 8 cycles; i2: 8 cycles; Rd2: 50 cycles) with an estimated sequencing depth of 5 x 10^4 reads per cell.

Analysis of single cell RNA-sequencing data

For droplet-based scRNA-seq data, the Cell Ranger software (v7.1.0, 10x Genomics) was used to demultiplex the BCL files into FASTQ files (cellranger mkfastq), to perform alignment (to Cell Ranger human genome GRCh38-2020-A), filtering and unique molecular identifier counting and to produce gene-barcode matrices. For microwell-based scRNA-seq data, the BCL files were demultiplexed into FASTQ files using Illumina Bcl2Fastq. The BeeNet pipeline software (v1.1, Honeycomb Biotechnologies) was used to process the raw data into count matrices, to perform alignment (to BeeNet human reference genome index from the GRCh38 Homo sapiens), filtering and unique molecular identifier counting and to produce gene-barcode matrices.

Filtered matrix files were used for further scRNA-seq analyses with R Bioconductor (v3.17) and Seurat (v4.3.0). Filtered matrices containing cell IDs and feature names in each sample were used to build a Seurat object. Features with fewer than 400 genes and 800 unique transcripts were removed and a threshold of < 20% mitochondrial reads was used to filter down to the final total cell numbers per sample for analysis. Alternatively, the threshold for genes was decreased to 100 genes instead of 400 genes. Gene counts in each sample were normalized separately by the default method ‘LogNormalize’ with a scale factor of 10,000. Two thousand highly variable features were identified with the ‘vst’ method. The 4 droplet samples and the 4 microwell samples were integrated together, with integration performed separately for each

AJRCMB Articles in Press. Published May 20, 2025 as 10.1165/rcmb.2024-0467MA

method, using FindIntegrationAnchors function (Seurat) with anchor.features = 2000. The reciprocal Principal Component Analysis (RPCA) integration method was used for batch effect correction. Cell doublets were identified and removed using scDblFinder. Cells were clustered using the FindClusters function (a resolution of 0.5 was selected, 15 PC were included in the umap). Eleven and thirteen clusters were identified in samples analysed with the microwell- vs. droplet-based platforms, respectively. Microwell and droplet datasets were also integrated together with RPCA.

To predict the regulatory potential of transcription factors in single cells, BALF cells analyzed by scRNA-seq were subjected to single-cell regulatory network inference and clustering (SCENIC) analysis (15). The normalized counts, nFeature_RNA and nCount_RNA in the merged Seurat object were used for the initial SCENIC analysis. The genes expressed with a value of 3 in 0.1% of the cells and detected in 1% of the cells were retained, and coexpression network analysis was made with GENIE3 in the SCENIC package. The 10 most specific markers of each cluster were selected using Regulon Specificity Scores, their regulon AUC scores were plotted in a heatmap (ComplexHeatmap).

AJRCMB Articles in Press. Published May 20, 2025 as 10.1165/rcmb.2024-0467MA

Supplemental Figures

AJRCMB Articles in Press. Published May 20, 2025 as 10.1165/rcmb.2024-0467MA

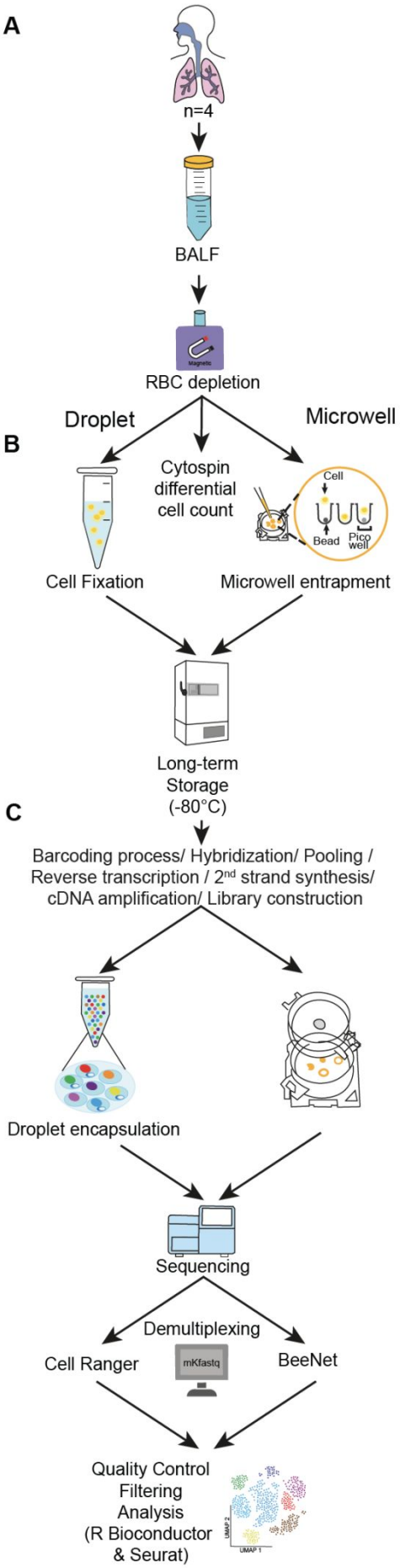

Figure E1. Overview of the experimental design. (*A*) Sample collection: BALFs were collected from 4 human donors during routine diagnostic procedures and BALF cells were depleted from red blood cells (RBC) via magnetic separation. (*B*) Cell fixation and cryopreservation. (*C*) Post-storage processing, sequencing and computational pipeline.

AJRCMB Articles in Press. Published May 20, 2025 as 10.1165/rcmb.2024-0467MA

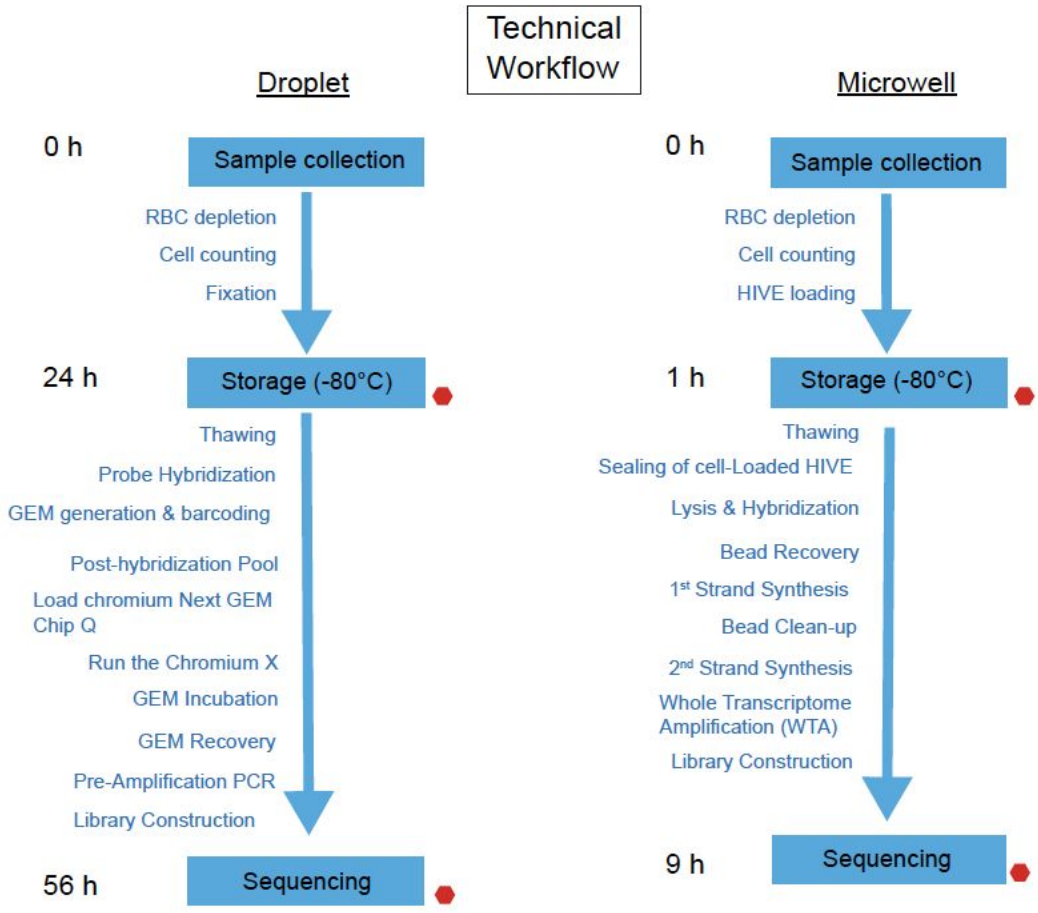

Figure E2. Technical workflow from sample collection to sequencing. The average times required until storage and sequencing are indicated. Red hexagons indicate steps where the protocol can be paused.

AJRCMB Articles in Press. Published May 20, 2025 as 10.1165/rcmb.2024-0467MA

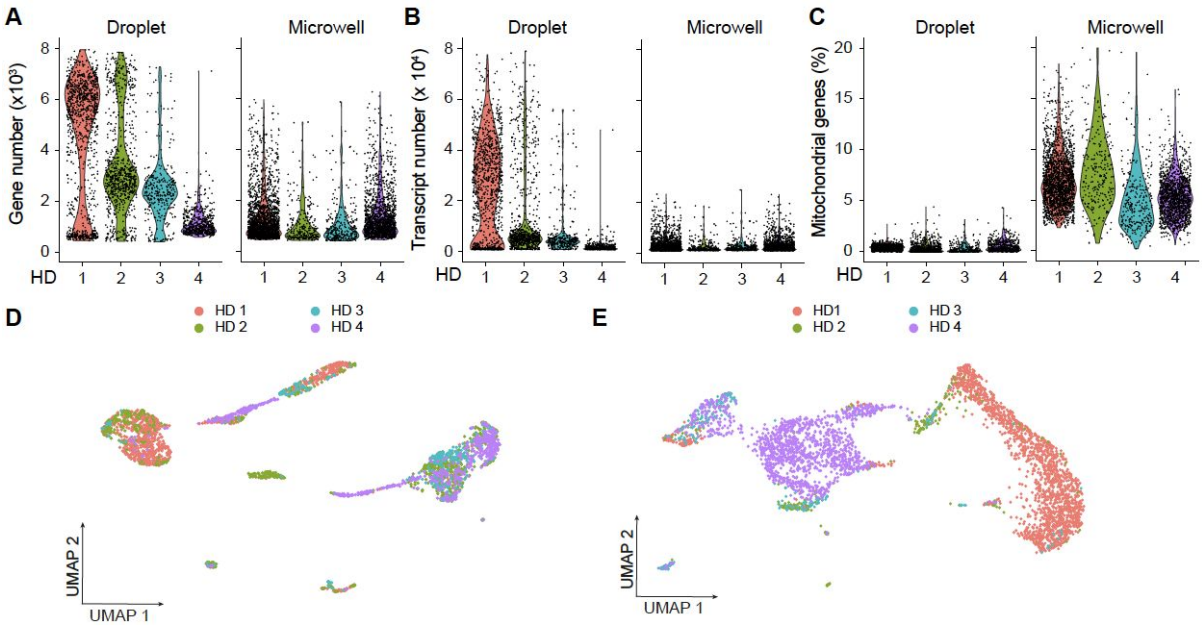

Figure E3. Human donor (HD)-specific distribution of gene and transcript numbers, mitochondrial gene percentages, and transcriptional identity of BALF cells. (*A*) Violin plot showing the number of genes detected in single cells for both methods, grouped by HD (height: gene number; width: abundance of cells). (*B*) Violin plot depicting the number of transcripts detected in single cells, as in (*A*). (*C*) Violin plot showing the percentage of mitochondrial genes detected in single cells, as in (*A*). (*D*) UMAP plot of droplet scRNA-seq data showing the transcriptional identity of BALF cells, annotated according to HD origin. (*E*) UMAP plot of microwell scRNA-seq data showing the transcriptional identity of BALF cells, annotated according to HD origin. Related to Figure 1.

AJRCMB Articles in Press. Published May 20, 2025 as 10.1165/rcmb.2024-0467MA

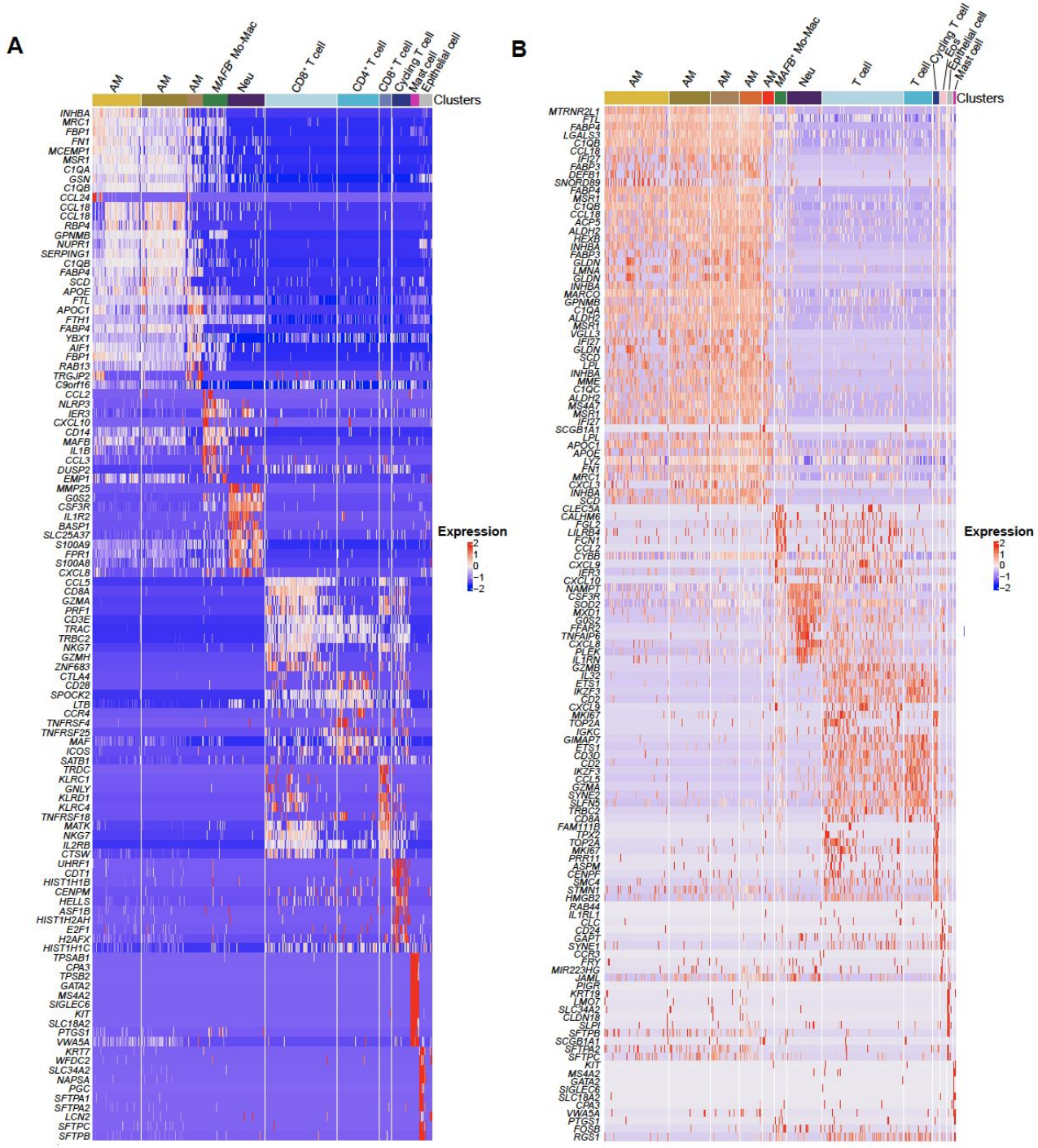

Figure E4. Heatmap showing the single-cell expression of the top ten most upregulated genes within each cluster of BALF cells analyzed by droplet (*A*) or microwell (*B*). Related to Figure 1.

AJRCMB Articles in Press. Published May 20, 2025 as 10.1165/rcmb.2024-0467MA

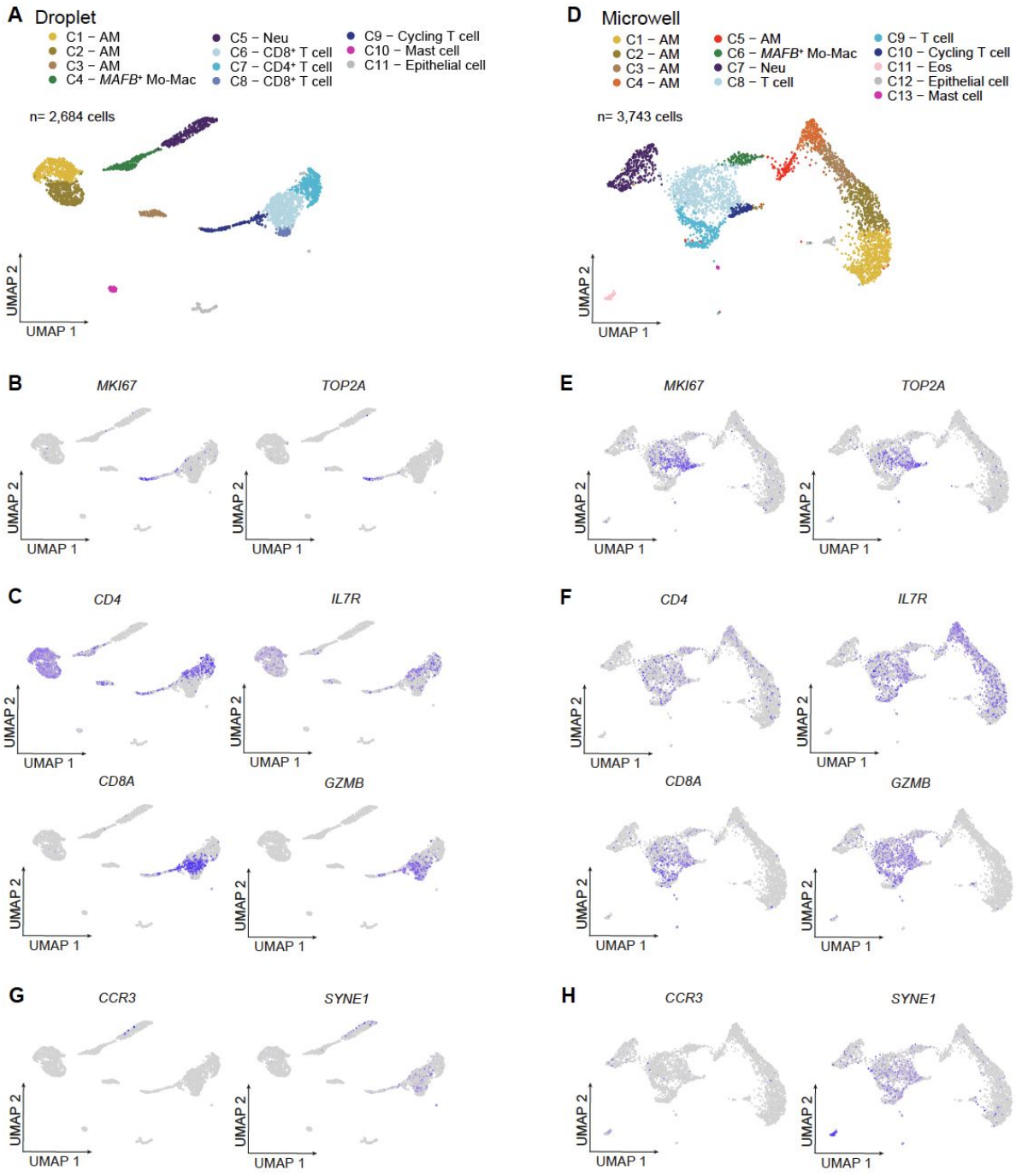

AJRCMB Articles in Press. Published May 20, 2025 as 10.1165/rcmb.2024-0467MA

Figure E5. Single cell expression of cell identity genes in droplet and microwell scRNA-seq data. (*A*) Uniform Manifold Approximation and Projection (UMAP) plots of droplet scRNA-seq data depicting the transcriptional identity of human BALF cells. (*D*) UMAP plots of microwell scRNA-seq data depicting the transcriptional identity of human BALF cells. *(B-H)* Feature plots displaying the expression level of cycling genes (*B,E*), T cell-related genes (*C,F*) and eosinophil-related genes (*G,H*) in single cells analyzed by droplet (*B,C,G*) and microwell (*E,F,H*).

AJRCMB Articles in Press. Published May 20, 2025 as 10.1165/rcmb.2024-0467MA

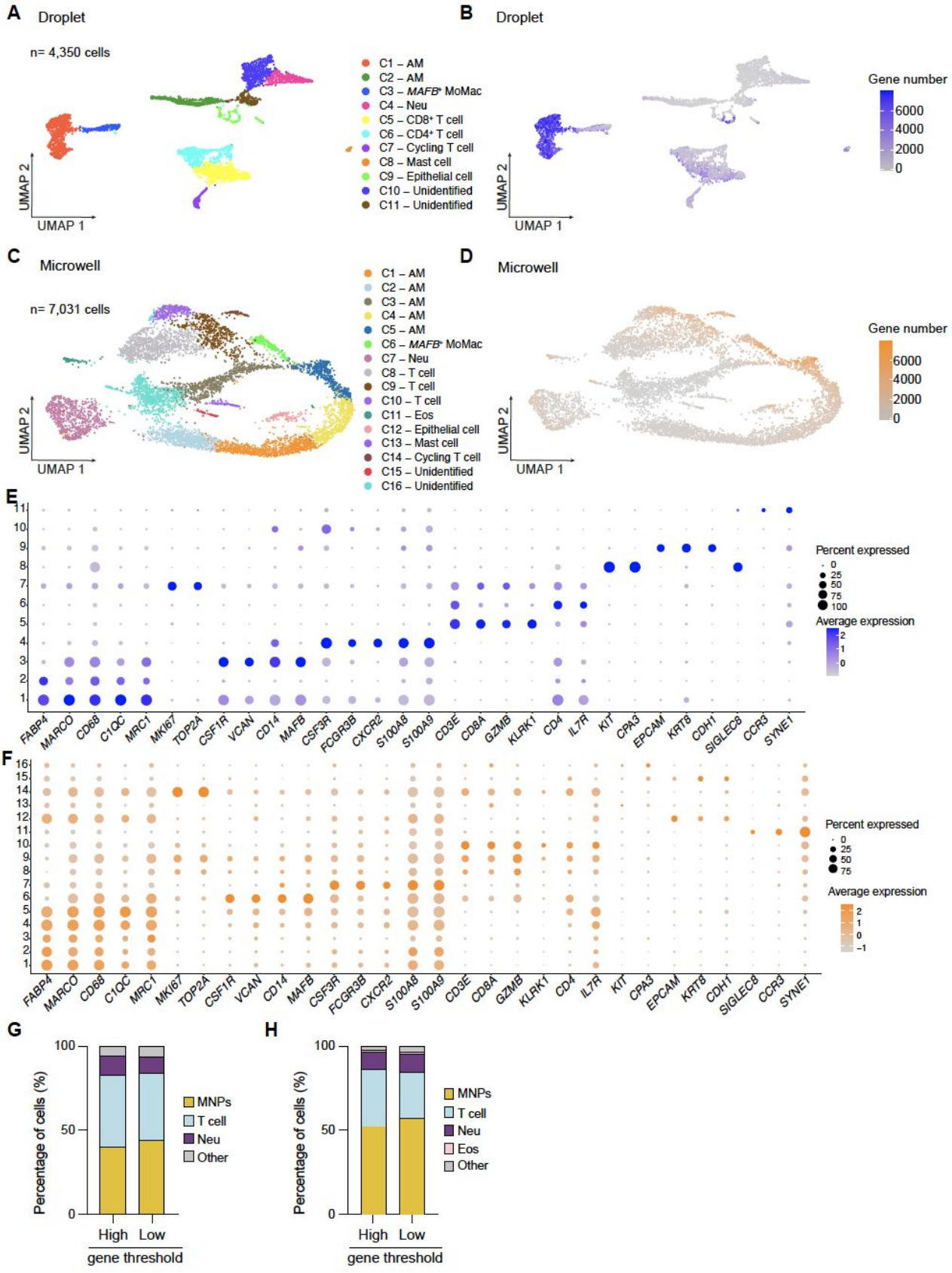

AJRCMB Articles in Press. Published May 20, 2025 as 10.1165/rcmb.2024-0467MA

Figure E6. Analysis of droplet and microwell scRNA-seq data with a lower threshold of at least 100 detected genes**.** *(A)* UMAP plots of droplet scRNA-seq data depicting the transcriptional identity of human BALF cells. (*B*) UMAP feature plot, as in (*A*), according to the number of detected genes. *(C)* UMAP plots of microwell scRNA-seq data depicting the transcriptional identity of human BALF cells. (*D*) UMAP feature plot, as in (*C*), according to the number of detected genes. (*E,F*) Dot plots displaying the average expression of specific genes and the percentage of cells expressing those genes within each cluster analyzed by droplet (*E*) and microwell *(F)*. (*G, H*) Bar graphs showing the frequency of the indicated cell populations analyzed by droplet (*G*) and microwell (*H*) with a high threshold (i.e., minimum 400 detected genes) and a low threshold (i.e., minimum 100 detected genes). AM, Alveolar Macrophage; Eos, Eosinophil; Mo-Mac, monocyte-derived macrophage; Neu, Neutrophil.

AJRCMB Articles in Press. Published May 20, 2025 as 10.1165/rcmb.2024-0467MA

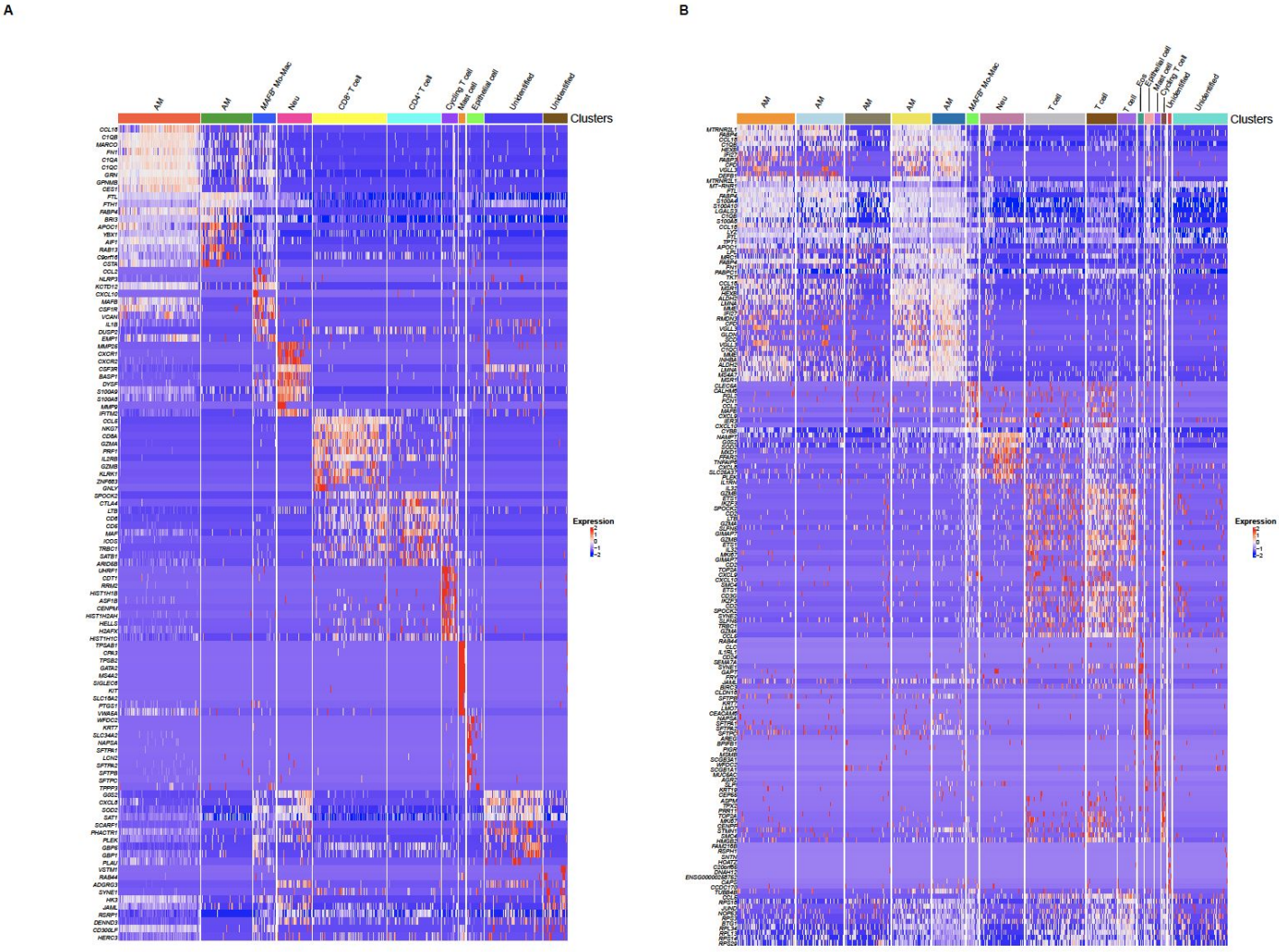

Figure E7. Heatmap showing the single-cell expression of the top ten most upregulated genes within each cluster of BALF cells analyzed by droplet (*A*) or microwell (*B*) with the threshold of detected genes lowered to 100 genes minimum. Related to Figure E6.

AJRCMB Articles in Press. Published May 20, 2025 as 10.1165/rcmb.2024-0467MA

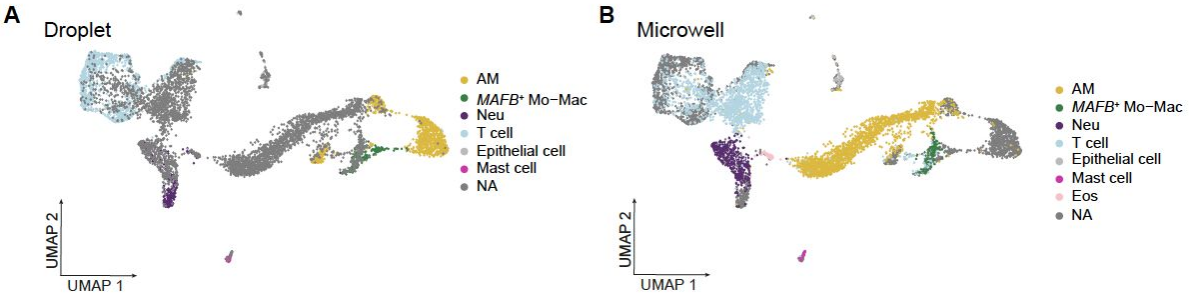

Figure E8. UMAP plots of integrated scRNA-seq data from droplet and microwell methods, highlighting the droplet (*A*) or the microwell (*B*) cells. AM, Alveolar Macrophage; Eos, Eosinophil; Mo-Mac, monocyte-derived macrophage; Neu, Neutrophil.

AJRCMB Articles in Press. Published May 20, 2025 as 10.1165/rcmb.2024-0467MA

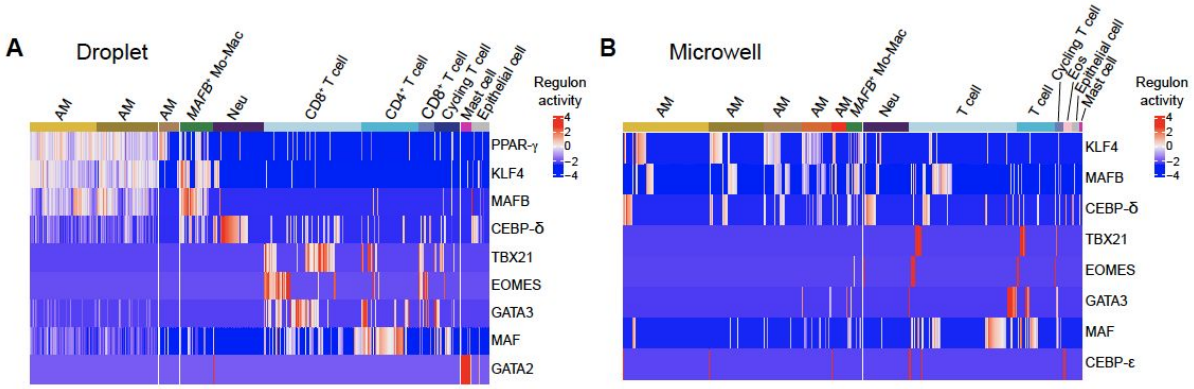

Figure E9. Heatmap showing the single-cell mRNA expression levels of transcription factors (TFs) within each cluster of BALF cells analyzed by droplet (*A*) or microwell (*B*).

AJRCMB Articles in Press. Published May 20, 2025 as 10.1165/rcmb.2024-0467MA

Supplemental Tables

Table E1. List of reagents and resources used in this study.

REAGENT or RESOURCE	SOURCE	IDENTIFIER
Antibodies		
4',6-diamidino-2-phénylindole (DAPI)	ThermoFisher	Cat#D3571
Propidium Iodide ultra-pure (PI)	Enzo life sciences	Cat#ENZ52403
Chemicals, Peptides and Recombinant Proteins		
Bovine Serum Albumin (BSA)	Sigma	Cat#A7906
DPBS	ThermoFisher	Cat#14190094
EDTA	Merck Millipore	Cat#1084181000
Fetal Bovine Serum (FBS)	Sigma	Cat#F7524
Formaldehyde 37%	Fisher	Cat#10532955
EasySep™ RBC Depletion Reagent	Stemcell Technologies	Cat#18170
Chromium Next GEM Single Cell Fixed RNA Sample Preparation kit, 16 rxns	10x Genomics	Cat#PN-1000414
Chromium Fixed RNA Kit, Human Transcriptome, 4 rxns x 16 BC	10x Genomics	Cat#PN-1000476
Chromium Next GEM Chip Q Single Cell Kit, 16 rxns	10x Genomics	Cat#PN-1000422
Glycerol for molecular biology, >99.0%	Sigma-Millipore	Cat#G5516-100ML
EasySep™ Magnet	Stemcell Technologies	Cat#18000

AJRCMB Articles in Press. Published May 20, 2025 as 10.1165/rcmb.2024-0467MA

HIVE™ Scout Kit	PerkinElmer	Cat#NOVA-HCB026
Trypan Blue Solution, 0.4%	ThermoFisher Scientific	Cat#15250061
UltraPure Bovine Serum Albumin (BSA, 50 mg/ml)	ThermoFisher Scientific	Cat#AM2616
DNA LoBind Tubes 2.0 ml	Eppendorf	Cat#022431048

Software and algorithms

Adobe Illustrator 2022	Adobe	
Cell Ranger	Cell Ranger Software	
BeeNet	BeeNet Software	https://download.honeycomb.bio/
Seurat	Seurat Software	https://satijalab.org/seurat/
Prism 10	GraphPad Software	https://www.graphpad.com/scientific-software/prism/

AJRCMB Articles in Press. Published May 20, 2025 as 10.1165/rcmb.2024-0467MA

Table E2. Transcript numbers, gene numbers and % of mitochondrial genes in BALF single cells analyzed by droplet and microwell. See Excel file.

AJRCMB Articles in Press. Published May 20, 2025 as 10.1165/rcmb.2024-0467MA